

Imaging of Corneal Neovascularization: Optical Coherence Tomography Angiography and Fluorescence Angiography

Matthias Brunner,^{1,2} Vito Romano,^{1,2} Bernhard Steger,³ Riccardo Vinciguerra,^{1,2} Samuel Lawman,² Bryan Williams,² Nicholas Hicks,¹ Gabriela Czanner,^{2,4} Yalin Zheng,² Colin E. Willoughby,^{1,2} and Stephen B. Kaye^{1,2}

¹Department of Corneal and External Eye Diseases, St. Paul's Eye Unit, Royal Liverpool University Hospital, Liverpool, United Kingdom

²Department of Eye and Vision Science, Institute of Ageing and Chronic Disease, University of Liverpool, Liverpool, United Kingdom

³Department of Ophthalmology, Medical University of Innsbruck, Innsbruck, Austria

⁴Department of Biostatistics, Institute of Translational Medicine, University of Liverpool, United Kingdom

Correspondence: Vito Romano, St. Paul's Eye Unit, Royal Liverpool University Hospital, 8Z Link, Prescot Street, Liverpool L7 8XP, UK; vito.romano@gmail.com.

MB and VR are joint first authors.

Submitted: April 11, 2017

Accepted: February 8, 2018

Citation: Brunner M, Romano V, Steger B, et al. Imaging of corneal neovascularization: optical coherence tomography angiography and fluorescence angiography. *Invest Ophthalmol Vis Sci*. 2018;59:1263–1269. <https://doi.org/10.1167/iovs.17-22035>

PURPOSE. The purpose of this study was to compare optical coherence tomography angiography (OCTA) and indocyanine green angiography (ICGA) for the assessment of corneal neovascularization (CoNV).

METHODS. Patients with CoNV extending at least 3 mm into the cornea were included. All patients underwent corneal imaging at the same visit. Images were recorded using the AngioVue OCTA system (Optovue, Inc.) with the long corneal adaptor module (CAM-L). ICGA images were recorded with fluorescent filters using the Heidelberg system (HRA2 Scanning Laser Ophthalmoscope; Heidelberg Engineering). Images were graded for quality by two independent observers. Vessel parameters: area, number, diameter, branch and end points, and tortuosity, were compared between devices. Bland-Altman plots were used to assess differences between parameters.

RESULTS. Fifteen patients with CoNV predominantly associated with microbial keratitis were included. Mean subjective image quality score was better for ICGA (3.3 ± 0.9) than for OCTA (2.1 ± 1.2 , $P = 0.002$), with almost perfect interobserver agreement for ICGA images ($\kappa = 0.83$) and substantial agreement for OCTA images ($\kappa = 0.69$). Agreement of grading of all investigated vessel parameters between ICGA and OCT images was slight to moderate, with significant differences found for vessel diameter ($-8.98 \mu\text{m}$, $P = 0.01$, 95% limits of agreement [LOA]: -15.89 to -2.07), number of branch (25.93 , $P = 0.09$, 95% LOA: -4.31 to 56.17), and terminal points (49 , $P = 0.05$, 95% LOA: 0.78 to 97.22).

CONCLUSION. Compared with ICGA, current OCTA systems are less precise in capturing small vessels in CoNV complexes, and validation studies are needed for OCTA segmentation software. OCTA, however, complements ICGA by providing evidence of red blood cell flow, which together with depth information, may be helpful when planning treatment of CoNV.

Keywords: corneal imaging, cornea neovascularization, optical coherence tomography angiography, fluorescence angiography, indocyanine green angiography

The human cornea in its healthy state is an avascular tissue, with the dynamic balance between pro- and antiangiogenic factors actively maintained by the inhibition of immune and inflammatory events.¹ A wide range of inflammatory, infectious, degenerative, and traumatic disorders may disturb this balance and lead to corneal neovascularization (CoNV). CoNV is associated with vision loss and is one of the main causes of corneal blindness, representing a major public health burden in developed countries.^{1,2} In the United States, the prevalence of CoNV is 4% in the general population, and the incidence per year is 1.4 million patients.³ CoNV also carries a risk of reduced graft survival following a corneal transplant.^{4,5}

Fluorescence angiography was recognized as a useful tool for the evaluation of diseased corneal vessels four decades ago.⁶ With the advent of new imaging systems and analytical processes, it has gained growing popularity in the clinical

assessment of CoNV.^{7–12} The combined use of fluorescein and indocyanine green angiography (FA and ICGA) has demonstrated better vessel delineation compared with biomicroscopy findings, particularly for vessels beneath areas of corneal scarring.⁷ In conjunction with objective computer-assisted image analysis, FA and ICGA provide a reliable method for assessing CoNV, such as the measurement of multiple vessel parameters and vessel maturity.¹³ Comparing CoNV quantitatively is a key requirement for guiding and evaluating treatment.¹³ Nevertheless, fluorescence angiography remains an invasive imaging technique, which is not only time-consuming and examiner dependent, but although rare, also carries the risk of adverse reactions, such as nausea and anaphylactic reactions.¹⁴

Optical coherence tomography (OCT) is a well-established noninvasive imaging technique that generates high-resolution



volumetric (three-dimensional) structural images.¹⁵ The axial resolution of the OCT image data is achieved by measuring the time of flight of light by utilizing its interference with light sent down a separate reference path. In early clinical OCT systems, this was done in time domain (TD) by scanning a mirror in the reference arm relative to the sample. When the reference path length matches a signal from the sample an interference pattern is generated. Modern clinical OCT systems are axially resolved in the Fourier domain (FD), which improves signal-to-noise ratio (SNR). In this case, the reference mirror is fixed, and the light is measured as a function of its frequency. The Fourier transform of the measured spectrum then gives the axially resolved signal. The lateral resolution of image data in current clinical OCT systems works in the same way as laser scanning confocal microscopy (LSCM), with a single image spot being laterally scanned across the sample. The three-dimensional data acquired by OCT can be used to reconstruct an en face view¹⁶ of coronal sections. OCT is also able to produce functional images of motion by measuring small changes between consecutive measurements. Quantification of blood flow by Doppler OCT has been studied since the early days of OCT.¹⁷ There are several methods of doing this including the Doppler shift of the interference fringes in TD systems and changes in the pixels Fourier phase between consecutive measurements in FD systems. The technical challenges in implementing such precise quantitative systems in a clinical environment, however, is likely to be the main factor in why it has not emerged commercially. The problem can be simplified to a near binary problem of just identifying where there is significant flow rather than trying to get an absolute measure of it. This is known as OCT-angiography (OCTA) and can be implemented by identifying areas where the OCT signal amplitude varies between consecutive images. OCTA has recently started emerging for clinical application.¹⁷ A major reason for this is the development of more robust processing methods, such as adding split spectrum decorrelation analysis that splits a FD signal into multiple lower axial resolution spectral bands before construction of separate OCT images for each band. The signal de-correlation between consecutive measurements is calculated for each band and then averaged. This gives a higher SNR of flow detection,¹⁸ which increases the methods robustness. Current clinical OCTA instruments are designed specifically for the retina due to the prevalence and clinical importance of blood vessels within its structure. The use of OCTA for ocular surface vessel analysis is currently at a clinical experimental stage.^{19–22}

The aim of this study was to evaluate and compare OCTA with fluorescence angiography for the evaluation of CoNV.

PATIENTS AND METHODS

Patients with clinically evident CoNV on biomicroscopy were prospectively recruited from the Department of Corneal and External Eye Disease, Royal Liverpool University Hospital, United Kingdom, between July and August 2016. Only one eye of each patient was investigated. In patients with bilateral CoNV, the eye with more extensive disease on biomicroscopy was imaged. Inclusion criteria were the presence of CoNV extending at least 3 mm into the cornea, with or without corneal scarring, infiltrate or oedema.

Exclusion criteria were less than 18 years of age, contradictions to undergoing ICGA such as allergies to iodine or shellfish, renal failure, or pregnancy, or the inability to fixate on a target due to blindness and/or continuous eye movements such as nystagmus. All patients underwent imaging (OCTA and ICGA) during the same visit. Demographics and clinical data (age, sex, involved eye, diagnosis, best-corrected visual acuity

[BCVA], location and duration of CoNV, and previous treatment) were included. The location of CoNV was assessed on slit-lamp biomicroscopy and was defined as superficial if vessels invaded the cornea in the anterior third of the corneal stroma and deep if vessels occurred in the mid and posterior third of the corneal stroma. The study received an Institutional Review Board approval from the ethical committee of The Royal Liverpool and Broadgreen University Hospital and was conducted according to the ethical standards set out in the 1964 Declaration of Helsinki, as revised in 2000. All patients provided informed consent.

OCTA

Images were recorded using the AngioVue OCTA system (Optovue, Inc., Fremont, CA, USA) with the long corneal adaptor module (CAM-L) as previously described.^{19,20,22} The device uses a light source centred on 840 nm and a bandwidth of 45 nm, giving an axial resolution of 5 μ m in tissue. The lateral beam width is 22 μ m and lateral sampling is 20 μ m. The A-scan rate is 70,000 per second. The device measures a three-dimensional scan cube of 6 \times 6 \times 2.3 mm. The images are processed using a split-spectrum amplitude de-correlation angiography (SSADA) algorithm.

After correct positioning of the patient at the device, three to six corneal scans were performed for each eye using the manual defocusing method and the AngioRetina scan mode. Following instructions from the instruments' manufacturer and in line with previous studies,^{19,22–24} the autofocus function was deactivated. After turning down the background illumination, the cornea adaptor lens was then moved toward the corneal surface by advancing the joystick until the corneal tissue appeared in the OCT window (approximately 2 to 3 cm). The focal lengths were manually specified by adjusting the manual F and Z settings (approximately -14 and $+14$ diopters [D]) until the vessels in the ROI were clearly in focus. Patients were instructed to fixate the target during the image acquisition and avoid blinking or eye movements during the scanning process.

ICGA

ICGA images were recorded with fluorescent filters before angiography, as red free, infrared, and fluorescent filters using the Heidelberg system (HRA2 Scanning Laser Ophthalmoscope; Heidelberg Engineering, Heidelberg, Germany) using a 15°, 20°, or 30° lens with a lens focus between 32 and 53 D. Following administration of 3 mL ICG, videography was undertaken for 60 seconds (early phase), commencing 10 seconds after the injection.^{7,8,13}

Image Analysis

The OCTA and ICGA images were independently graded for the appearance of dye in ICGA images and vessel visibility in OCTA images by two masked observers (VR and RV) using a subjective image quality score (0 to 4) as previously published (0 = no vessel discernible, 1 = poor vessel delineation, 2 = good vessel delineation, 3 = very good vessel delineation, 4 = excellent vessel delineation).⁷ For the OCTA images, the signal strength index (SSI) was recorded (Optovue uses a proprietary SSI to indicate the signal strength [image quality] of OCT scans on a scale from 0 to 100 [higher is better]). The best ICGA (late frames with complete filling of afferent and efferent vessels) and OCTA images were selected and exported in BMP format for the purpose of semiautomated quantitative image analysis.

In a first step, the pixel resolution (mm/pixel) of the selected ICGA images was defined by using the corneal

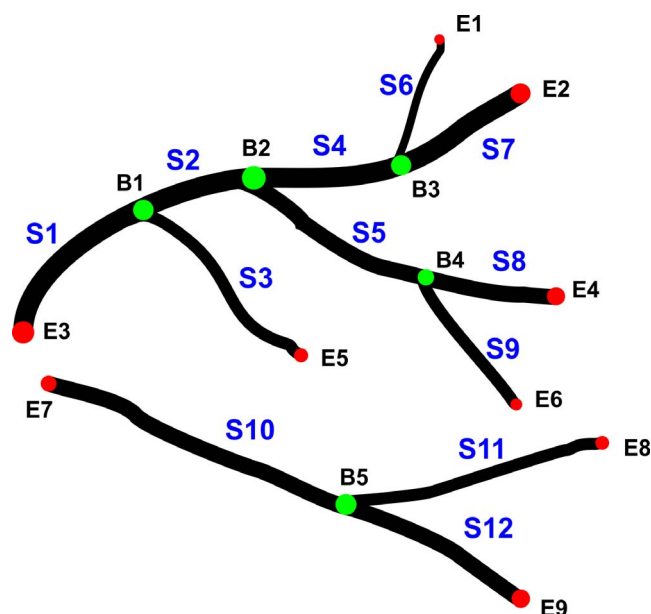


FIGURE 1. Diagram showing the vessel parameters. In the diagram, branch points B_i are represented by green circles and end points E_i by red circles. Vessel segment S_i is the vessel between either two branch points or between a branch point and an end point. In the diagram, there are five branch points, nine end points, and 12 segments. For each segment, the diameter of a vessel segment is defined as the average diameter measured along its path. The number of pixels belonging to vessels is used to estimate the area of vessels. Please note, in this diagram, vessel pixels are in black and background is in white for the best print effect.

diameter (12 mm) as reference distance.⁷ In a second step, two landmarks on the ICGA image under consideration were chosen to define a circular region of interest (ROI) with them as the end points of its diameter. The same landmarks were used to define a ROI on the OCTA image while the pixel resolution of the OCTA image can be derived from the distance between the two landmarks. This standardization process will make these two ROIs almost cover the same area of the cornea, and only vessels within them will be analyzed and compared in the following step.

In a third step, an in-house automated programme written in Matlab R2016a 64-bit (The Mathworks, Inc., Natick, MA, USA) was used to detect and analysed the vessels. This programme is based on Ref. 7 but has been significantly improved with a more robust extensively validated segmentation algorithm.²⁵ More specifically, the eigen-value based filter was replaced by a local phase based filter for (universal) optimal enhancement effect on images with large variations and computation efficiency. To improve the connectivity of the segmented vessels, an infinite perimeter active contour model was used to partition the enhanced image into a binary image (vessel pixels, 1; background, 0). A diagram showing the vessel parameters is shown in Figure 1 and an example of vessel segmentation is shown in Figure 2. The segmented vessels within the ROI were analyzed further to extract parameters characterizing the vasculature by following.⁷ For example, branch point is defined as the location where vessel bifurcates, whereas end point is where a vessel terminates. A vessel segment is defined between either two branch points or between a branch point and an end point. The diameter of a vessel segment is defined as the average diameter measured along its path. Parameters, such as vessel area, vessel diameter, number of branch points, and end points, were compared between OCTA and ICGA. All the above analyses were

performed on a computer (configurations: Windows7 Service Pack 1 [Microsoft Corporation, Redmond, WA, USA], Intel Xeon CPU-E5 [Intel Corporation, Mountain View, CA, USA], 3.0 GHz, and 32 GB of RAM). For demarcation and depth localization of CoNV on cross-sectional OCTA scans, the cornea was divided into an anterior, mid-, and posterior portion. A scale bar was added to the images by dividing the corneal thickness at the apex into three sections of equal height.

Statistical Analysis

Quantitative measurements were reported as mean \pm SD and minimum, median, and maximum. Boxplots were used to assess normality of data. Wilcoxon rank-signed tests were used to test for differences. P values of less than 0.05 were considered statistically significant. Bland-Altman plots were used to assess agreement between vessel parameter measurements of OCTA and ICGA images and the mean of those observed differences, with 95% limits of agreement (LOA) and with 95% confidence interval for LOA are reported.^{22,26} Cohen's κ statistic was used to test the levels of agreement between the image quality scores from two observers. Interpretation of levels of agreement was based on that recommended for two (binary) categories for each patient.²⁷ At a value of ≤ 0.2 , κ was considered slight, $0.2 < \kappa \leq 0.4$ was considered fair; $0.4 < \kappa \leq 0.6$ was considered moderate, $0.6 < \kappa \leq 0.8$ was considered substantial, and $\kappa > 0.8$ was considered as almost perfect.

RESULTS

Seventeen patients were recruited. Two patients were excluded due to poor gaze fixation and resultant poor quality OCTA images. Fifteen patients (median age, 61 years; range, 29 to 78 years; male-to-female ratio, 8:7) were included with a mean duration of CoNV of 35 ± 41.7 months (median, 18 months; range, 3 to 141 months). The patient demographics and clinical features are summarized in Table 1.

Nine eyes had apparent superficial CoNV and six eyes deep CoNV demonstrated by OCTA (Fig. 3). The mean total vessel area of CoNV was larger using ICGA compared with OCTA ($P = 0.02$) and in only 53% of cases (8 of 15) did the OCTA capture all of the CoNV area. The mean subjective quality scores for ICGA and OCTA images were 3.3 ± 0.9 and 2.1 ± 1.2 ($P = 0.002$), respectively (Fig. 4). Interobserver agreement for the image quality scores was almost perfect for ICGA images (weighted Cohen's $\kappa = 0.83$) and substantial for OCTA images (weighted Cohen's $\kappa = 0.69$). The mean signal strength index for OCTA images was 26.4 ± 9.8 (min-max, 7 to 42). The signal strength index was poorer in eyes with corneal scarring ($P = 0.002$) and deep CoNV ($P = 0.008$), compared with those without scarring and superficial vessels (Fig. 5A). The image quality score in eyes with CoNV plus scarring and eyes with deep CoNV was found to be significantly better using ICGA compared with OCTA ($P = 0.009$ and $P = 0.03$, respectively). Overview images of the entire cornea could only be acquired with ICGA due to the limited field of view with OCTA (Fig. 5B).

An overview of the vessel parameter measurements is summarized in Table 2. Higher values were measured for all parameters obtained from ICGA images compared with OCTA images, except for the mean vessel diameter, which was significantly higher in OCTA images (40.75 vs. $49.73 \mu\text{m}$, $P = 0.01$). Significant differences were also found for the number of terminal points (119.27 vs. 70.27 , $P = 0.01$). The mean differences and limits of agreement are outlined in Table 3. Significant mean differences (measurement bias) were found

TABLE 1. Patient Demographics and Clinical Data

Patient No. (Sex, Laterality)	Age (y)	Diagnosis	Duration of CoNV (mo)	Area of CoNV (Quadrants)	Location of CoNV	Corneal Scarring	Treatment for CoNV*	BCVA (logMAR)
1 (F, OS)	35	Rosacea keratitis	>6	1	Superficial	Yes	FND	0.2
2 (F, OD)	79	LSCD	>6	4	Superficial and deep	No	Topical steroids	1
3 (F, OD)	54	HSK	>6	1	Superficial	Yes	Topical steroids	0.8
4 (F, OD)	61	HSK	>6	2	Superficial and deep	Yes	FND	0.8
5 (F, OS)	69	HSK	>6	3	Superficial and deep	Yes	FND	0.6
6 (M, OS)	68	LSCD	>6	2	Superficial	No	Topical steroids	0.2
7 (M, OS)	62	PK (corneal dystrophy)	>6	2	Superficial	No	FND	0.2
8 (M, OS)	71	Rosacea keratitis	>6	1	Superficial	Yes	FND	0.3
9 (F, OS)	39	HSK	>6	1	Superficial	Yes	Topical steroids	0.2
10 (M, OD)	46	Rosacea keratitis	>6	2	Superficial and deep	Yes	FND	0.3
11 (M, OS)	62	HSK	>6	1	Superficial and deep	Yes	Topical steroids	1.0
12 (F, OD)	62	LSCD	>6	1	Superficial and deep	Yes	Topical steroids	NPL
13 (M, OD)	31	PK (graft rejection)	3–6	1	Superficial	No	Topical steroids	0.3
14 (M, OD)	52	PK, HSK	3–6	2	Superficial	No	Topical steroids	0.2
15 (M, OS)	29	Contact lens-related	3–6	1	Superficial	No	None	−0.1

See Figure 2 for vessel depth location on OCTA. Deep CoNV, vessels located in mid to posterior third the stroma on biomicroscopy; F, female; FND, fine needle diathermy; HSK, herpes simplex keratitis; LSCD, limbal stem cell deficiency; M, male; NPL, no perception of light; OD, right eye; OS, left eye; PK, penetrating keratoplasty; superficial CoNV, vessels in the subepithelium and anterior third of stroma, on biomicroscopy.

* All patients received topical steroids before and after FND treatment.

for vessel diameters ($-8.98 \mu\text{m}$, $P = 0.01$, 95% LOA, -15.89 to -2.07), number of branch points (25.93 , $P = 0.05$, 95% LOA -4.31 to 56.17), and number of terminal points (49 , $P = 0.05$, 95% LOA 0.78 to 97.22), when comparing ICGA and OCTA images. The variability of the total number of vessels increased with increasing number of vessels (see Supplementary Data: Bland-Altman plots).

DISCUSSION

Both the quantitative and qualitative assessment of CoNV are prerequisites for disease monitoring and planning of treatment. The biomicroscopic assessment of CoNV, although very useful,

has several limitations for identifying and quantifying CoNV, especially in the presence of scarring. Previous reports have demonstrated that fluorescence angiography (ICGA) not only allows better vessel delineation than biomicroscopy but provides information on the vessel maturity of CoNV and also enables the differentiation between afferent and efferent vessels, which is critical for the planning of treatment such as selective vessel occlusion with fine needle diathermy.^{7,8,13}

OCTA is an emerging and promising new technique for noninvasive angiographic imaging. It detects blood vessels by the temporal variances in amplitude and/or phase of the OCT signal due to movement of red blood cells.^{28,29} Current commercial available OCTA systems have been designed for retinal vessel analysis and have been successfully used in the assessment of various vascular pathologies of the posterior

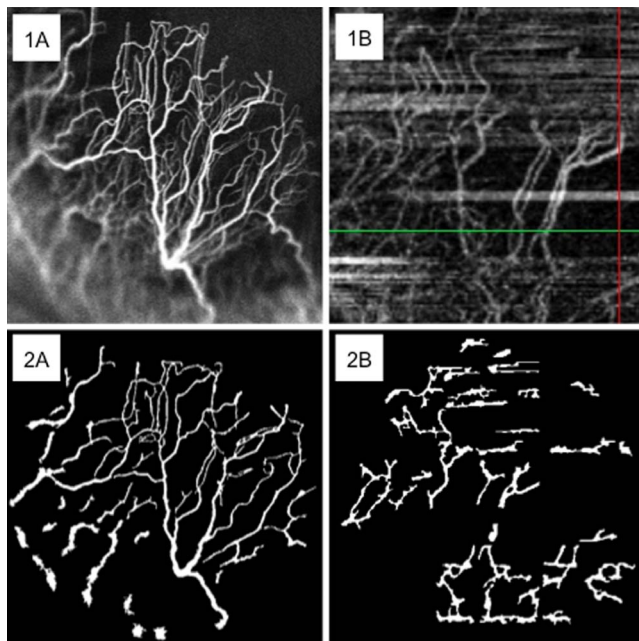


FIGURE 2. (1A) ICGA. (1B) OCTA. (2A) Segmentation of ICGA. (2B) Segmentation of OCTA.

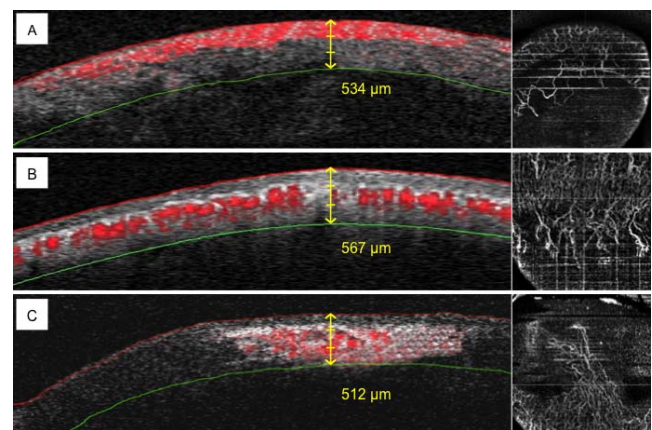


FIGURE 3. Cross-sectional OCTA scans (left) demonstrating corneal neovascularization (erythrocyte flow highlighted in red) at different corneal depths (anterior, mid, or posterior), and corresponding coronal OCTA scans (right). (A) Superficial vessels located at the level of epithelium and anterior third of the corneal stroma at the graft-host interface in a patient with penetrating keratoplasty (Table 1, patient 7). (B) Deep vessels located in the mid stroma in a patient with recurrent HSK (Table 1, patient 14). (C) Deep vessels located in the mid and posterior third of the corneal stroma in a patient with rosacea keratitis and concomitant corneal scarring (Table 1, patient 1).

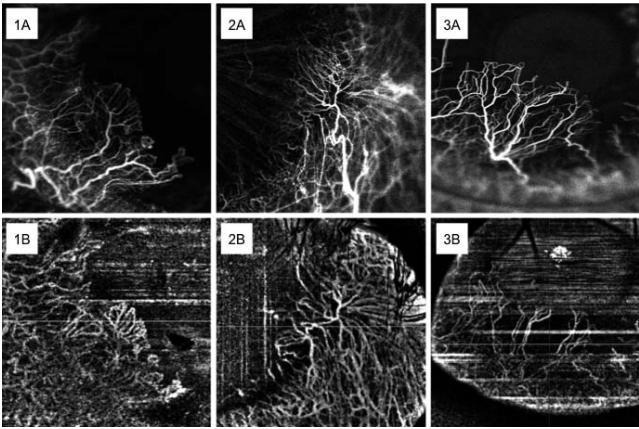


FIGURE 4. (1–3A) ICGA images (20° lens, focus 32 D) of CoNV secondary to herpes simplex keratitis (Table 1, patient 3, 1A) and rosacea keratitis (Table 1, patients 8 and 10, 2A and 3A). (1–3B) Corresponding OCTA images (6 × 6-mm scan size) of the same eyes.

segment.^{23,24,30,31} In conjunction with a corneal optical adaptor lens, the same systems can be used for angiographic anterior segment imaging.^{19–22} The location of the anterior and posterior interfaces of the cornea are found by image segmentation, which can then be used to select manifolds of set corneal depths. To increase the SNR ratio, a range of corneal depths can be averaged. This coronal reconstruction process allows for an instant overview of the corneal pathology and changes to the length, caliber, and area of CoNV, which is not possible with B-scan OCT views alone.³² Coronal scans may also provide information on the depth of invading corneal vessels.

The current literature on OCTA for the anterior segment use, however, is sparse.^{19–22} A previous study by Ang et al.²⁰ compared area of CoNV measurements between OCTA and ICGA in eight patients and found good agreement with comparable results for both imaging techniques. In this study, we analyzed various vessel parameters to further investigate and better compare OCTA with ICGA for imaging of CoNV. We found slight to moderate agreement between all investigated vessel parameters, including the mean overall area of CoNV, suggesting that the two imaging methods are currently not interchangeable but may complement each other. OCTA and ICGA imaging, however, is observer dependent, and possible measurement bias due to differences in observer experience in capturing OCTA images with the AngioVue device needs to be considered. OCTA images were of significantly lower quality compared with ICGA images ($P = 0.002$; Fig. 4). OCTA was less accurate in capturing smaller and more distal vessels of the neovascular networks. Markedly fewer numbers of vessels, branch points, and end points were detected with OCTA than

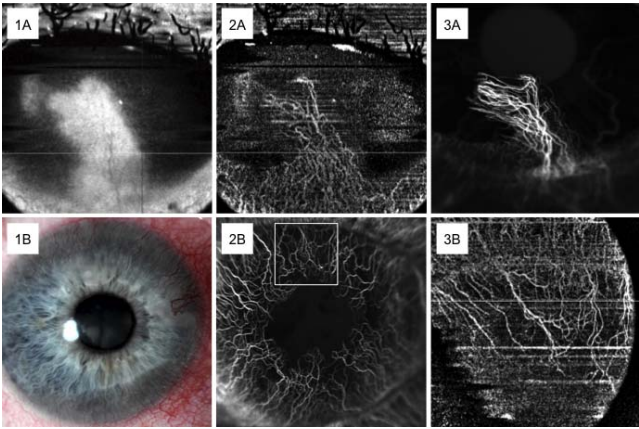


FIGURE 5. (1–3A) Vascularized corneal scar in an eye of a 35-year-old female patient with rosacea keratitis (Table 1, patient 1). Red free OCT image (1A), OCTA (6 × 6-mm scan size, 2A), and ICGA (0:17.03, 20° lens, 32 D focus, 2C). (1–3B) A 79-year-old female patient with limbal stem cell deficiency and 360° of CoNV (Table 1, patient 2). Color image (1B), ICGA (1:02.22, 30° lens, 32 D focus, 2B), and OCTA (6 × 6-mm scan size; 3B). Note the comparably small field width in the OCTA image.

with ICGA, which is likely to account for the significant differences in the mean diameter ($P = 0.01$) and total number of terminal points ($P = 0.01$) between the two imaging methods. In fact, the mean vessel diameter was the only parameter to show significantly higher values with OCTA compared with ICGA, which may be explained by the fact that a smaller mean overall number of vessels captured by OCTA compared with ICGA and that OCTA performed less well in capturing smaller size. OCTA is dependent on the movement of cells, and the images of vessels do not represent the actual lumen, but movement of erythrocytes; their movement is used to reconstruct the morphologic appearance of blood vessels.^{28,33–35} Potential reasons for the poorer performance of the current OCTA system, compared with ICGA, are that the motion of erythrocytes may be reduced or absent in vessels with very small diameters in corneal neovascular networks, thereby limiting vessel delineation. In addition, the lateral resolution is limited, and there are artifacts caused by light scatter, gradient of corneal curvature, and patient eye movements or blinking during image acquisition. Current technical issues, which should be rapidly overcome, are limitations of current image processing algorithms, the need for instrumentation refinement, such as wider field of view, improvement of eye tracking and reinclusion of auto focus, and increased user expertise. A limitation of this and other studies using OCTA for CoNV is that the software used for deriving vessel parameters such as segmentation has not been directly

TABLE 2. Summary of Vessel Parameters

Parameter	ICGA		OCTA		P Value*
	Mean (SD)	Min, Max (Med)	Mean (SD)	Min, Max (Med)	
Total vessel area (mm ²)	1.92 (1.40)	0.25, 4.17 (1.85)	1.65 (2.68)	0.10, 9.52 (0.61)	0.10
Number of vessels (<i>n</i>)	123.67 (77.24)	20, 267 (119)	83.53 (95.09)	9, 320 (44)	0.08
Branch points (<i>n</i>)	69.40 (42.63)	11.68, 142 (68)	43.47 (52.01)	4, 180 (18)	0.06
Terminal points (<i>n</i>)	119.27 (81.50)	25, 299 (98)	70.27 (67.43)	8, 232 (41)	0.01
Mean vessel diameter (μm)	40.75 (9.70)	23.30, 57.80 (39.80)	49.73 (14.72)	25.40, 77.70 (48.40)	0.01
Mean vessel tortuosity	1.11 (0.05)	1.10, 1.30 (1.10)	1.09 (0.05)	1.00, 1.20 (1.10)	0.20

n = 15 eyes.
* Wilcoxon nonparametric signed-rank test.

TABLE 3. Agreement of Vessel Measurements Between ICGA and OCTA

Parameter	Mean Difference ICGA-OCTA	SD	95% CI for Mean Difference	P Value	95% LOA	95% CI	
						Lower LOA	Upper LOA
Total vessel area (mm ²)	0.27	2.02	−0.85 to 1.38	0.62	−3.69 to 4.22	−5.62 to −1.75	2.29 to 6.16
Number of vessels (n)	40.13	101.43	−16.04 to 96.31	0.15	−158.68 to 238.95	−255.97 to −61.38	141.65 to 336.24
Branch points (n)	25.93	54.61	−4.31 to 56.17	0.09	−81.10 to 132.97	−133.48 to −28.72	80.59 to 185.34
Terminal points (n)	49.00	87.08	0.78 to 97.22	0.05	−121.67 to 219.67	−205.19 to −38.15	136.15 to 303.19
Mean vessel diameter (μm)	−8.98	12.48	−15.89 to −2.07	0.01	−33.44 to 15.48	−45.41 to −21.47	3.51 to 27.45
Mean vessel tortuosity	0.02	0.07	−0.02 to 0.57	0.27	−0.11 to 0.15	−0.18 to −0.05	0.09 to 0.22

n = 15 eyes.

validated for anterior segment OCT (AS-OCTA). Although the software we used has been validated and shown to be robust and accurate for corneal ICG and fluorescein angiography,^{7–13} validation studies for AS-OCTA for CoNV are needed, and therefore, these results need to be treated with caution.

The OCTA images in our series showed more artifacts in eyes with CoNV in the presence of scarring or exudates. Also, the signal strength index of the OCTA images was lower in our cohort than previously reported in two studies (26.4 ± 9.8 vs. 38 ± 14 and 36.95 ± 13.97 , respectively),^{20,22} possibly due to differences of clinical presentation of CoNV and the cooperation of patients, which may have also influenced our results. It is of note that to obtain good images patients need to maintain fixation for several seconds, which they at times found difficult.

A main disadvantage of the current AngioVue OCTA system, however, is the limited field of view, which is restricted to 6×6 mm. In seven eyes, it was not possible to image the full extent of CoNV with a single scan (Fig. 5B). This is an important requirement particularly for monitoring disease, which is achieved with ICGA by the use of different angle lenses with the Heidelberg Spectralis system, thereby allowing flexible field of view adjustments during the imaging process. A similar process would be indicated for OCTA to make OCTA images comparable.

Although conventional fluorescence angiography (FA and ICGA) has shown to be a very useful imaging technique to quantitatively and functionally assess CoNV, lymphatic, and ghost vessels it has several disadvantages.^{9–11,36} It is time consuming and requires intravenous dye injection, it is contraindicated in pregnant patients or patients with significantly impaired liver and kidney function, and it may cause adverse events such as nausea and less commonly allergic or anaphylactic reactions. In contrast, the potential advantages of noncontact and dye-free OCTA are obvious: the technique allows rapid angiographic image acquisition, is easy to use, and avoids the need for cannulation and the risk of dye-associated side effects. Although not capable of differentiating between active and inactive vessels and to identify afferent efferent vessels as in the case of conventional fluorescence (FA and ICG) angiography,¹⁰ OCTA enables three-dimensional imaging with more depth information than conventional fluorescence angiography, thus potentially providing more objective information on the localisation of CoNV. This may be important for monitoring purposes and of benefit when planning for surgical procedures such as diathermy or anterior lamellar keratoplasty.²² Although stereo images using ICGA and or FA provides some depth information, they are not easily quantifiable.⁷

A key advantage of OCTA may be its suitability for serial angiographic imaging. A recent case series compared before and after treatment imaging after a variety of interventions and reported promising results that support the potential role of OCTA for monitoring changes in corneal vascular areas.²¹

Moreover, OCTA may be used to quantify flow rates of erythrocytes within vessels in neovascular networks as a novel objective biomarker for assessing CoNV. At present, OCTA is limited by methodical and technical issues, described above, causing vessel duplication, residual motion lines and vessel discontinuity, compared with convention angiography, that often make the OCTA images difficult to interpret. The most striking artifacts present in all the OCTA images are line artifacts. If the patient moves, or blinks, during a B-scan (fast axis), the OCTA method fails and gives false motion at all positions on this plane (slow axis). The AngioVue device can collect the OCT data sets (registration of data sets will be by a proprietary algorithm) using alternate fast and slow axes leading to orthogonal line artifacts being present in some images, particularly Figure 2B. Errors in the segmentation, due to these false signals, are visible in Figure 5 bottom left.

In conclusion, OCTA is a promising new imaging technique for CoNV, but our data suggest that the current instrument on its own is not sufficient for characterizing and monitoring CoNV. Further technological improvements in OCTA and optimized image processing algorithms are needed to improve image quality and reduce projection, shadow, and motion artifacts, and software validation studies are needed. Combining OCTA with conventional fluorescence angiography in a multimodal approach, however, may improve monitoring of disease and treatment planning but this will require longitudinal studies.

Acknowledgments

Disclosure: **M. Brunner**, None; **V. Romano**, None; **B. Steger**, None; **R. Vinciguerra**, None; **S. Lawman**, None; **B. Williams**, None; **N. Hicks**, None; **G. Czanner**, None; **Y. Zheng**, None; **C.E. Willoughby**, None; **S.B. Kaye**, None

References

1. Azar DT. Corneal angiogenic privilege: angiogenic and antiangiogenic factors in corneal avascularity, vasculogenesis, and wound healing (an American Ophthalmological Society thesis). *Trans Am Ophthalmol Soc.* 2006;104:264–302.
2. Dana MR, Streilein JW. Loss and restoration of immune privilege in eyes with corneal neovascularization. *Invest Ophthalmol Vis Sci.* 1996;37:2485–2494.
3. Lee P, Wang CC, Adamis AP. Ocular neovascularization: an epidemiologic review. *Surv Ophthalmol.* 1998;43:245–269.
4. Bachmann B, Taylor RS, Cursiefen C. Corneal neovascularization as a risk factor for graft failure and rejection after keratoplasty: an evidence-based meta-analysis. *Ophthalmology.* 2010;117:1300–1305.
5. The Collaborative Corneal Transplantation Studies Research Group. The collaborative corneal transplantation studies (CCTS). Effectiveness of histocompatibility matching in

- high-risk corneal transplantation. *Arch Ophthalmol*. 1992; 110:1392-1403.
6. Easty DL, Bron AJ. Fluorescein angiography of the anterior segment. Its value in corneal disease. *Br J Ophthalmol*. 1971; 55:671-682.
 7. Anijeet DR, Zheng Y, Tey A, Hodson M, Sueke H, Kaye SB. Imaging and evaluation of corneal vascularization using fluorescein and indocyanine green angiography. *Invest Ophthalmol Vis Sci*. 2012;53:650-658.
 8. Spiteri N, Romano V, Zheng Y, et al. Corneal angiography for guiding and evaluating fine-needle diathermy treatment of corneal neovascularization. *Ophthalmology*. 2015;122:1079-1084.
 9. Romano V, Steger B, Brunner M, Ahmad S, Willoughby CE, Kaye SB. Method for angiographically guided fine-needle diathermy in the treatment of corneal neovascularization. *Cornea*. 2016;35:1029-1032.
 10. Steger B, Romano V, Kaye SB. Corneal indocyanine green angiography to guide medical and surgical management of corneal neovascularization. *Cornea*. 2016;35:41-45.
 11. Romano V, Steger B, Zheng Y, Ahmad S, Willoughby CE, Kaye SB. Angiographic and in vivo confocal microscopic characterization of human corneal blood and presumed lymphatic neovascularization: a pilot study. *Cornea*. 2015;34:1459-1465.
 12. Steger B, Romano V, Kaye SB. Angiographic evaluation of inflammation in atopic keratoconjunctivitis [published online ahead of print November 30, 2016]. *Ocular Immunol Inflamm*. doi:10.1080/09273948.2016.1247873.
 13. Kirwan RP, Zheng Y, Tey A, Anijeet D, Sueke H, Kaye SB. Quantifying changes in corneal neovascularization using fluorescein and indocyanine green angiography. *Am J Ophthalmol*. 2012;154:850-858.
 14. Stanga PE, Lim JJ, Hamilton P. Indocyanine green angiography in chorioretinal diseases: indications and interpretation: an evidence-based update. *Ophthalmology*. 2003;110:15-21.
 15. Huang D, Swanson EA, Lin CP, et al. Optical coherence tomography. *Science*. 1991;254:1178-1181.
 16. Wojtkowski M, Srinivasan V, Fujimoto JG, et al. Three-dimensional retinal imaging with high-speed ultrahigh-resolution optical coherence tomography. *Ophthalmology*. 2005; 112:1734-1746.
 17. Leitgeb RA, Werkmeister RM, Blatter C, Schmetterer L. Doppler optical coherence tomography. *Progr Retinal Eye Res*. 2014;41:26-43.
 18. Jia Y, Tan O, Tokayer J, et al. Split-spectrum amplitude-decorrelation angiography with optical coherence tomography. *Optics Express*. 2012;20:4710-4725.
 19. Ang M, Sim DA, Keane PA, et al. Optical coherence tomography angiography for anterior segment vasculature imaging. *Ophthalmology*. 2015;122:1740-1747.
 20. Ang M, Cai Y, MacPhee B, et al. Optical coherence tomography angiography and indocyanine green angiography for corneal vascularisation. *Br J Ophthalmol*. 2016;100:1557-1563.
 21. Cai Y, Alio Del Barrio JL, Wilkins MR, Ang M. Serial optical coherence tomography angiography for corneal vascularization. *Graefes Arch Clin Exp Ophthalmol*. 2017;255:135-139.
 22. Ang M, Cai Y, Shahipasand S, et al. En face optical coherence tomography angiography for corneal neovascularisation. *Br J Ophthalmol*. 2016;100:616-621.
 23. Jia Y, Bailey ST, Wilson DJ, et al. Quantitative optical coherence tomography angiography of choroidal neovascularization in age-related macular degeneration. *Ophthalmology*. 2014;121:1435-1444.
 24. Spaide RF, Klancnik JM Jr, Cooney MJ. Retinal vascular layers imaged by fluorescein angiography and optical coherence tomography angiography. *JAMA Ophthalmol*. 2015;133:45-50.
 25. Zhao Y, Rada L, Chen K, Harding SP, Zheng Y. Automated vessel segmentation using infinite perimeter active contour model with hybrid region information with application to retinal images. *IEEE Trans Med Imaging*. 2015;34:1797-1807.
 26. Bland JM, Altman DG. Statistical methods for assessing agreement between two methods of clinical measurement. *Lancet*. 1986;1:307-310.
 27. Viera AJ, Garrett JM. Understanding interobserver agreement: the kappa statistic. *Family Med*. 2005;37:360-363.
 28. de Carlo TE, Romano A, Waheed NK, Duker JS. A review of optical coherence tomography angiography (OCTA). *Int J Retina Vitreous*. 2015;1:5.
 29. Tahiri Joutei Hassani R, Liang H, El Sanharawi M, et al. En-face optical coherence tomography as a novel tool for exploring the ocular surface: a pilot comparative study to conventional B-scans and in vivo confocal microscopy. *Ocular Surface*. 2014;12:285-306.
 30. Jia Y, Wei E, Wang X, et al. Optical coherence tomography angiography of optic disc perfusion in glaucoma. *Ophthalmology*. 2014;121:1322-1332.
 31. de Carlo TE, Bonini Filho MA, Chin AT, et al. Spectral-domain optical coherence tomography angiography of choroidal neovascularization. *Ophthalmology*. 2015;122:1228-1238.
 32. Lathrop KL, Gupta D, Kagemann L, Schuman JS, Sundarraj N. Optical coherence tomography as a rapid, accurate, noncontact method of visualizing the palisades of Vogt. *Invest Ophthalmol Vis Sci*. 2012;53:1381-1387.
 33. Motaghiannezam R, Fraser S. Logarithmic intensity and speckle-based motion contrast methods for human retinal vasculature visualization using swept source optical coherence tomography. *Biomed Optics Express*. 2012;3:503-521.
 34. Wang RK, Jacques SL, Ma Z, Hurst S, Hanson SR, Gruber A. Three dimensional optical angiography. *Optics Express*. 2007; 15:4083-4097.
 35. Ren H, Du C, Park K, Volkow ND, Pan Y. Quantitative imaging of red blood cell velocity in vivo using optical coherence Doppler tomography. *Appl Physics Lett*. 2012;100:233702-233704.
 36. Zheng Y, Kaye AE, Boker A, et al. Marginal corneal vascular arcades. *Invest Ophthalmol Vis Sci*. 2013;54:7470-7477.